

## Positronium Formation and Diffusion in a Molecular Solid Studied with Variable-Energy Positrons

M. Eldrup,<sup>(a)</sup> A. Vehanen,<sup>(b)</sup> Peter J. Schultz, and K. G. Lynn  
*Brookhaven National Laboratory, Upton, New York 11973*

(Received 20 July 1983)

Crystalline and amorphous ice were studied with monoenergetic positrons with incident energies  $0 < E < 5$  keV. Positronium (Ps) forms in the ice and diffuses as a neutral particle until annihilation or escape from the surface. Measurement of the fraction of *o*-Ps leaving the surface reveals two distinct contributions to the total Ps-formation probability (both Ore- and spur-type) as well as the Ps diffusion coefficient,  $0.17 \pm 0.09$  cm<sup>2</sup>/sec in crystalline ice. In addition, positronium trapping is observed in sputtered (crystalline) ice and voids ( $\geq 17$  Å diameter) in amorphous ice.

PACS numbers: 78.70.Bj, 61.70.Ey, 71.60.+z, 82.55.Gm

During the last few years the development of beams of low-energy ( $< 10$ -keV) positrons has opened up new fields of research of surface and near-surface phenomena in metals and semiconductors.<sup>1</sup> In this Letter we report on the first low-energy positron study of a molecular crystal, designed to obtain information about positronium (Ps) formation, diffusion, and interactions with structural defects. Ice, studied extensively before,<sup>2,3</sup> was chosen as the first substance. Positrons injected into ice (and many other insulators) may form Ps, a bound positron-electron state. The formation process has been under strong debate.<sup>4,5</sup> In the Ore model the positron—when reaching energies in a range typically 5–10 eV (the Ore gap) during slowing down—ionizes a molecule with simultaneous formation of a Ps atom.<sup>4</sup> In the spur model Ps formation takes place between the thermalized positron and a thermalized excess electron.<sup>5</sup> This excess electron is one of the species (ions, radicals, electrons) created inside the region called a spur when the positron loses its last major amount of energy (up to roughly 100 eV).<sup>5</sup> The different characteristic energies expected for the two models suggest that a differentiation between them can be made by a measurement of the Ps yield versus positron energy. Ps formed in ice may diffuse back to the surface and escape. By measurement of the fraction of escaping Ps versus the incident positron energy the Ps diffusion coefficient  $D_{\text{Ps}}$  can be determined. The few published  $D_{\text{Ps}}$  values for solids scatter over several orders of magnitude.<sup>4</sup>

The slow positron beam used is described elsewhere.<sup>6</sup> The ice samples were prepared in a UHV chamber by vapor deposition of triply distilled, degassed water onto a cold single-crystal Cd surface. Samples of crystalline ice were made with

a deposition rate of roughly  $0.5$  μm/min on a surface at 150 K, while for amorphous samples the rate was about  $0.05$  μm/min at 50 K.<sup>7</sup> Sample thicknesses were about  $10$  μm. The sample could be rotated towards the water vapor inlet or a sputtering gun. The annihilation radiation that is used to determine the orthopositronium (*o*-Ps) fraction was detected with an intrinsic Ge detector.

In ice Ps annihilates mainly with the emission of two (511-keV)  $\gamma$  quanta. In vacuum, *o*-Ps decays by  $3\gamma$  annihilation ( $E < 511$  keV), while *p*-Ps decays by  $2\gamma$  emission. Hence, the fraction of detected  $3\gamma$  events measures the amount of *o*-Ps escaping the sample (when corrected for the small fraction of  $3\gamma$  events from the bulk). This fraction,  $F_{3\gamma}$ , can be determined from the shape of the  $\gamma$ -energy spectrum.<sup>1,8,9</sup> Because of the repulsive exchange interaction between Ps and the surrounding molecules the Ps atom has a negative affinity to the crystal,<sup>10</sup> which is estimated<sup>11,12</sup> to be  $-2 \pm 1$  eV. Thus all Ps reaching the surface is expected to escape into vacuum. However, thermalized positrons in ice, which may also diffuse to the surface, cannot form Ps (unlike in most metals), because the lowest electron ionization energy ( $\approx 10$  eV)<sup>13</sup> is higher than the Ps binding energy ( $= 6.8$  eV), and the positron work function is measured to be positive. Thus the measured  $F_{3\gamma}$  is only due to Ps which formed inside or near the surface of the sample and subsequently escaped into vacuum.

Figure 1 shows a typical curve for  $F_{3\gamma}$  versus incident positron energy for crystalline ice at 150 K. Small differences between different samples were observed but the main characteristics remained the same, viz. (1) a low-energy part ( $E < 50$  eV) where  $F_{3\gamma}$  varies strongly and exhibits sharp maxima and minima (a similar structure

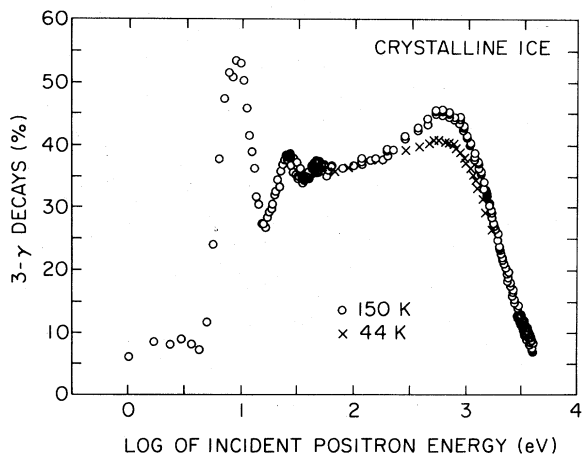


FIG. 1. Typical curves for the  $3\gamma$  annihilation fraction  $F_{3\gamma}$  of  $o$ -Ps vs  $\log_{10}$  of incident positron energy in crystalline ice. Some of the positrons in ice form Ps, which then diffuses to the surface and escapes into vacuum, where  $o$ -Ps annihilates with  $3\gamma$  emission.

was observed for mica by Mills<sup>1</sup>, (2) an intermediate region ( $50 < E < 700$  eV) where  $F_{3\gamma}$  has a slow, gradual increase, and (3) a high-energy region ( $E > 700$  eV) where  $F_{3\gamma}$  shows a steady decrease.

For ice the limits of the main Ore gap (i.e., that associated with the lowest ionization energy) can be estimated at<sup>4,13</sup>  $5 \pm 1$  to  $10 \pm 1$  eV. Taking into account that the curve in Fig. 1 is shifted 2–3 eV because of the charging of the crystal (by the positrons), the main peak is seen to fall exactly in the Ore gap. We interpret this peak as Ps formation resulting from an Ore-type process. The second peak (at  $\approx 25$  eV) is ascribed partly to positrons which have been scattered into the main Ore gap by one inelastic collision (in a few cases two), partly to an Ore gap at about 25–30 eV,<sup>13</sup> and partly to Ps formation by the spur mechanism for positron energies above the ionization threshold [ $\approx 10$  eV (Ref. 13)]. A more detailed discussion of this will be published elsewhere.<sup>12</sup>

As noted earlier, all Ps formed close to the surface will escape. Hence, above the oscillatory behavior, the measured  $F_{3\gamma} \approx 37\%$  represents the total  $o$ -Ps yield at  $E \approx 50$  eV. Bulk ice measurements<sup>2</sup> show an  $o$ -Ps yield of about 55%. Hence we ascribe the increase of  $F_{3\gamma}$  between 50 and 700 eV to the increase of the total Ps yield with incident positron energy. This increase is attributed to recombinations of thermalized positrons and electrons (i.e., a spur process). The number of ionized electrons generated by a posi-

tron increases with the incident energy. The range of the electrons until thermalization is expected to be about  $300 \text{ \AA}$ ,<sup>14</sup> i.e., roughly the same as the mean penetration depth of 1-keV positrons. Hence, the number of thermalized electrons, with which the positron has a nonzero probability to recombine into Ps, increases with initial positron energy up to roughly 1 keV, above which it does not change. Furthermore, the fraction of ionized electrons lost through the surface as secondary electrons (about 2 per incident positron at these energies<sup>15</sup>) becomes smaller with increasing incident positron energy. The decrease of  $F_{3\gamma}$  at  $E > 700$  eV is ascribed to the diffusion of Ps from the bulk to the surface in competition with the annihilation of Ps. This is analogous to positron diffusion results for metals.<sup>1,8</sup>

The measured curves above 50 eV were fitted by a model:

$$F_{3\gamma} = P(E) \{ F_0 [1 + (E/E_0)^n]^{-1} \}, \quad (1)$$

where

$$P(E) = (P_0 - P_{\text{max}}) \exp[-\frac{1}{2}(E/E_p)^\beta] + P_{\text{max}}$$

is an empirical expression for the energy-dependent Ps yield ( $= P_0$  at  $\approx 50$  eV,  $P_{\text{max}}$  in the bulk). The expression in curly brackets in Eq. (1) is derived from a one-dimensional diffusion model<sup>8</sup> giving the fraction of  $o$ -Ps that diffuses back to the surface (where it escapes). The mean penetration depth of positrons  $\bar{x}$ , and hence the mean Ps formation depth, is related<sup>1</sup> to the positron energy  $E$  approximately as  $\bar{x} = AE^n$ . Assuming that the slowing down of positrons is very similar to that of electrons, we can take  $A = 320 \pm 100 \text{ \AA/keV}^n$ .<sup>1,14,16</sup> The parameter  $E_0$  in Eq. (1) is related to the diffusion length  $L_{o\text{-Ps}}$  [ $L_{o\text{-Ps}} = (D_{\text{Ps}}\tau_{o\text{-Ps}})^{1/2} = AE_0^n$ , where  $\tau_{o\text{-Ps}} = 0.7$  nsec is the  $o$ -Ps lifetime in ice].

Table I gives the parameters extracted by the curve fitting for two different samples at given temperatures. For simplicity we give the value  $E_{1/2}$  at which  $P(E_{1/2}) = (P_{\text{max}} - P_0)/2 + P_0$ . The values of  $n$  in Table I are in reasonable agreement with the expected value of about 1.75.<sup>14</sup> Since the fitting parameters ( $E_0, n$ ) in the curly brackets in Eq. (1) are determined mainly from the data points at the highest energies, and since the empirical expression for  $P(E)$  can fit any reasonable, increasing curve that saturates, the fitted diffusion parameters depend only slightly on the functional form of  $P(E)$ . Still, there is a relatively strong correlation between  $n$  and  $E_0$ , which

TABLE I. The main parameters resulting from a fit of Eq. (1) to curves in Fig. 1 measured for two different samples ( $E > 50$  eV). The value of  $P_0$  is  $(49.5 \pm 2.5)\%$ . During fitting, two parameters were fixed,  $F_0 = 0.75$  and  $P_{\max} = 75\%$ . The uncertainties given in the table are estimates based on the scatter of the data of several runs (only one run at 70 K).  $E_{1/2}$  is the energy at which half the Ps yield increase has taken place.

$T$ (K)	$E_{1/2}$ (eV)	$E_0$ (eV)	$n$	$D_{Ps}$ ( $\text{cm}^2/\text{sec}$ )
44	$513 \pm 60$	$1830 \pm 30$	$1.73 \pm 0.02$	$0.12 \pm 0.01$
129	$369 \pm 30$	$2088 \pm 30$	$2.12 \pm 0.02$	$0.33 \pm 0.01$
147	$319 \pm 20$	$2067 \pm 13$	$2.14 \pm 0.03$	$0.33 \pm 0.02$
43	$549 \pm 40$	$1698 \pm 3$	$1.76 \pm 0.08$	$0.10 \pm 0.01$
70	558	1708	1.79	0.10
94	$554 \pm 13$	$1637 \pm 6$	$1.73 \pm 0.08$	$0.08 \pm 0.01$
125	$518 \pm 12$	$1722 \pm 21$	$1.89 \pm 0.03$	$0.12 \pm 0.01$
150	$434 \pm 20$	$1770 \pm 26$	$1.97 \pm 0.05$	$0.14 \pm 0.02$

may be reflected in the apparent temperature dependence of  $n$  and the scatter of  $E_0$  (Table I). From the present data we conclude that  $D_{Ps}$  in ice is  $0.17 \pm 0.09 \text{ cm}^2/\text{sec}$  with a relatively weak temperature dependence. This may be explained with a simple quantum-tunneling model of Ps diffusion, with a Ps bandwidth of about 1 eV. For comparison,  $D_{Ps}$  may be indirectly estimated, from the width of the  $p$ -Ps peaks in angular correlation curves.<sup>4</sup> Based on the high-resolution data of Douglas *et al.*<sup>17</sup> we obtain a rough estimate  $D_{Ps} \approx 0.3 \text{ cm}^2/\text{sec}$ .

The temperature effect clearly seen in Fig. 1 and in the decrease of  $E_{1/2}$  with temperature (Table I) is attributed mainly to the temperature dependence of the secondary-electron slowing down range due to a decrease of the electron mean free path between inelastic collisions.<sup>18</sup> Using the theory of Ref. 18 with a typical optical phonon energy in ice ( $200 \text{ cm}^{-1}$ ), we obtain a variation of the secondary-electron range very similar to that of  $E_{1/2}$ , i.e., only a small change up to about 100 K, and then a decrease to roughly 80% of the low-temperature value at 150 K.

To investigate the effect of surface damage, crystalline ice was bombarded at 44 K with 3-keV  $\text{Ne}^+$  ions that create damage in a 50–100-Å-thick surface layer. Figure 2 shows the strong effect of the damage, partly a result of inhibition of Ps formation in the bulk and partly due to Ps trapping in the defects created.<sup>2</sup> On annealing above approximately 100 K (the vacancy migration tem-

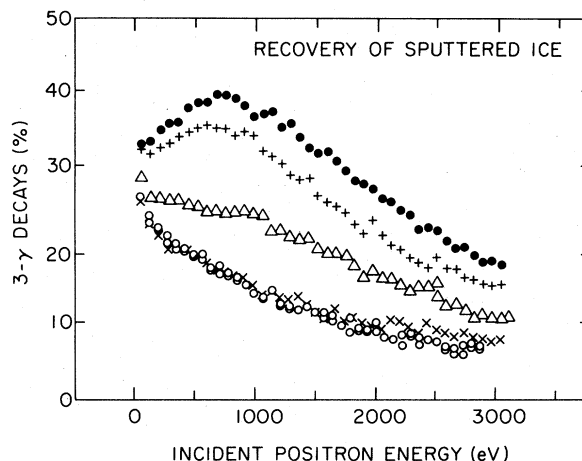


FIG. 2.  $F_{3\gamma}$  vs incident energy in crystalline ice after  $\text{Ne}^+$  sputtering and subsequent annealing. Open circles, as sputtered, 44 K; crosses, 50–117 K; triangles, 118–137 K; pluses, 137–145 K; solid circles, 145–149 K.

perature<sup>2</sup>) the curve characteristic of crystalline ice is gradually recovered.

Results obtained for amorphous ice are shown in Fig. 3. The curve for the as-grown sample differs significantly from the crystalline-ice curve (Fig. 2). There is a rapid initial decrease in  $F_{3\gamma}$  probably due to the much shorter  $L_{Ps}$  caused by Ps trapping in the amorphous structure.  $F_{3\gamma}$  levels off at (8–9)% for high positron energies. This shows that positrons penetrating as deep as  $(3-4) \times 10^3 \text{ \AA}$  have a rather large probability of  $3\gamma$  decay. This can only be explained by  $o$ -Ps trapping in large cavities in the bulk amorphous ice, where the pick-off annihilation

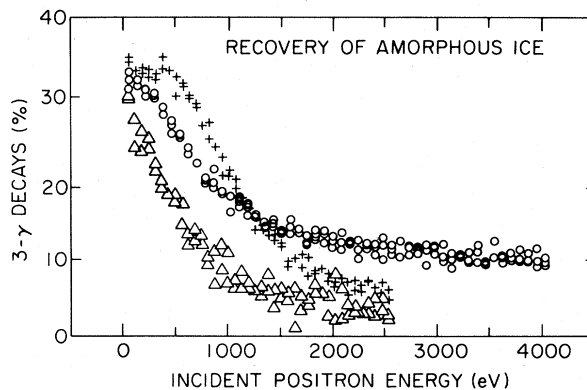


FIG. 3.  $F_{3\gamma}$  vs incident energy during annealing of amorphous ice. Open circles, as grown, 45 K; triangles, 115–132 K; pluses, 141–151 K. Major changes in the curve shapes occurred at 96–114 and 132–140 K.

rate is strongly reduced. If about 50% *o*-Ps is formed, all of which becomes trapped in cavities, there is roughly 17% probability of  $3\gamma$  annihilation. This leads to an *o*-Ps lifetime of  $0.17 \times 142 = 24$  nsec, equivalent to a cavity diameter of about  $17 \text{ \AA}$ .<sup>10</sup> On annealing above 100 K a clear transition takes place. The high-energy level of  $F_{3\gamma}$  disappears, signaling the disappearance of the cavities. At the amorphous-to-crystalline ice transition at 135 K (Ref. 3) the curve changes again. The variation of  $F_{3\gamma}$  with  $E$  is now consistent with the results for crystalline ice (Figs. 1 and 2), if the  $L_{Ps}$  is considerably shortened (to about  $150 \text{ \AA}$  compared to  $1000 \text{ \AA}$  in the as-grown crystal). This may be due to defects created at the phase transition that are capable of trapping Ps.

In conclusion, we have shown that Ps formation in crystalline ice apparently takes place via both an Ore-type process (seen for initial positron energies of 5–35 eV) and a spur-type process (seen for energies  $\geq 100$  eV). The Ps diffusion coefficient is determined to be  $0.17 \pm 0.09 \text{ cm}^2/\text{sec}$ , being the first direct measurement of diffusion of a neutral ultralight particle. A clear effect of near-surface damage was observed as well as a qualitative difference between crystalline and amorphous ice, the latter apparently containing large ( $\approx 17\text{-\AA}$ ) cavities in the as-grown state.

We thank O. E. Mogensen, F. M. Jacobsen, J. Schou, R. Nieminen, and I. K. MacKenzie for discussions. Two of us (M.E. and A.V.) thank their colleagues for the collaboration and hospitality during their stay at Brookhaven National Laboratory. This work was supported in part by the Division of Materials Sciences, U. S. Department of Energy, under Contract No. DE-AC02-76CH00016.

<sup>(a)</sup>Visitor from Risø National Laboratory, DK-4000 Roskilde, Denmark.

<sup>(b)</sup>Visitor from Helsinki University of Technology, SF-02150 Espoo 15, Finland.

<sup>1</sup>A. P. Mills, Jr., in *Positron Solid State Physics*, edited by W. Brandt and A. Dupasquier (North-Holland, Amsterdam, 1983); K. G. Lynn, *ibid.*

<sup>2</sup>O. E. Mogensen and M. Eldrup, *J. Glaciol.* **21**, 85 (1978); M. Eldrup, O. E. Mogensen, and J. H. Bilgram, *J. Glaciol.* **21**, 101 (1978).

<sup>3</sup>P. V. Hobbs, *Ice Physics* (Clarendon, Oxford, 1974).

<sup>4</sup>A. Dupasquier, in Ref. 1.

<sup>5</sup>O. E. Mogensen, in *Positron Annihilation*, edited by P. Coleman, S. Sharma, and L. M. Diana (North-Holland, Amsterdam, 1982), p. 763.

<sup>6</sup>K. G. Lynn and H. Lutz, *Rev. Sci. Instrum.* **51**, 977 (1980).

<sup>7</sup>S. A. Rice, W. G. Madden, R. McGraw, M. G. Sceats, and M. S. Bergren, *J. Glaciol.* **21**, 509 (1978).

<sup>8</sup>K. G. Lynn and D. O. Welch, *Phys. Rev. B* **22**, 99 (1980).

<sup>9</sup>Notice that in the present paper  $F_{3\gamma}$  is for *o*-Ps only, i.e., at most = 0.75, while  $F$  in the formulas in Refs. 1 and 8 is normalized to include *p*-Ps as well (assumed to have a yield one third of *o*-Ps), and hence  $0 \leq F \leq 1$ .

<sup>10</sup>M. Eldrup, in Ref. 5, p. 753.

<sup>11</sup>M. Eldrup, thesis, Risø Report No. 254, 1972 (unpublished).

<sup>12</sup>M. Eldrup, A. Vehanen, P. J. Schultz, and K. G. Lynn, to be published.

<sup>13</sup>R. A. Rosenberg, V. Rehn, V. O. Jones, A. K. Green, C. C. Parks, G. Loubriel, and R. H. Stulen, *Chem. Phys. Lett.* **80**, 488 (1981).

<sup>14</sup>J. Schou, thesis, Risø Report No. 391, 1979 (unpublished); H. Sørensen and J. Schou, *J. Appl. Phys.* **49**, 5311 (1978), and references therein.

<sup>15</sup>T. L. Matskewich and E. G. Mikhailova, *Fiz. Tverd. Tela* **2**, 709 (1960) [*Sov. Phys. Solid State* **2**, 655 (1960)].

<sup>16</sup>A. Adams and P. K. Hansma, *Phys. Rev. B* **22**, 4258 (1980).

<sup>17</sup>R. J. Douglas, M. Eldrup, L. Lupton, and A. T. Stewart, in *Positron Annihilation*, edited by R. R. Hasiguti and K. Fujiwara (Sendai, Japan, 1979), p. 621.

<sup>18</sup>A. J. Dekker, *Phys. Rev.* **92**, 1179 (1954).